

Statistical Modeling and Analysis of Mobile-to-Mobile Fading Channels in Cooperative Networks Under Line-of-Sight Conditions

Batool Talha · Matthias Pätzold

Published online: 9 April 2009
© Springer Science+Business Media, LLC. 2009

Abstract Recently, mobile-to-mobile (M2M) cooperative network technology has gained considerable attention for its promise of enhanced system performance with increased mobility support. As this is a new research field, little is known about the statistical properties of M2M fading channels in cooperative networks. So far, M2M fading channels have mainly been modeled under the assumption of non-line-of-sight (NLOS) conditions. In this paper, we propose a new model for M2M fading channels in amplify-and-forward relay links, where it is assumed that a line-of-sight (LOS) component exists in the direct link between the source mobile station and the destination mobile station. Analytical expressions will be derived for the main statistical quantities of the channel envelope, such as the mean value, variance, probability density function (PDF), level-crossing rate (LCR), and average duration of fades (ADF) as well as the channel phase. Our results show that the statistical properties of the proposed M2M channel are quite different from those of double Rayleigh and double Rice channels. In addition, a high-performance channel simulator will be presented for the new M2M channel model. The developed channel simulator is used to confirm the correctness of all obtained theoretical results by simulations.

Keywords Mobile-to-mobile fading channels · Cooperative networks · Amplify-and-forward relaying · Channel modeling · Level-crossing rate · Average duration of fades

The material in this paper is based on “On the Statistical Properties of Mobile-to-Mobile Fading Channels in Cooperative Networks Under Line-of-Sight Conditions”, by Batool Talha and Matthias Pätzold which appeared in the proceedings of the 10th International Symposium on Wireless Personal Multimedia Communications, WPMC 2007, Jaipur, India, December 2007.

B. Talha (✉) · M. Pätzold
Faculty of Engineering and Science, University of Agder, P. O. Box 509, 4898 Grimstad, Norway
e-mail: batool.talha@uia.no

M. Pätzold
e-mail: matthias.paetzold@uia.no

1 Introduction

M2M communications in cooperative wireless networks is an emerging technology. Combining the advantages of cooperative diversity [1–3] with the features of M2M communication systems [4] makes it possible to fulfill the consumer demands of enhanced quality of service (QoS) with greater mobility support. M2M cooperative wireless networks exploit the fact that single-antenna mobile stations can share their antennas to create a virtual multiple-input multiple-output (MIMO) system in a multi-user scenario [5]. Thus, such wireless networks permit mobile stations to relay signals using other mobile stations in the network to a final destination [6]. Furthermore, the mobile relays can either decode and retransmit the received signal or simply amplify and forward the signal [3]. This paper focuses on amplify-and-forward relay type M2M cooperative wireless networks.

Since M2M cooperative network technology is a rather new concept, there are only some few results available, which describe the multipath fading channel characteristics under some specific communication scenarios. Studies on the statistical properties of amplify-and-forward relay fading channels under NLOS conditions can be found in [7]. The authors of [7] have modeled the amplify-and-forward relay channel in the equivalent complex baseband as a zero-mean complex double Gaussian channel, i.e., the product of two zero-mean complex Gaussian channels. Hence, the envelope of the overall amplify-and-forward relay fading channel follows the double Rayleigh distribution [8]. Questions like how does the double Rayleigh fading impact the systems' performance are answered in [9]. However, there is still a lack of information about amplify-and-forward relay fading channels under LOS conditions. Thus, the purpose of this paper is to fill this gap by analyzing the statistical properties of amplify-and-forward relay fading channels under LOS conditions.

An LOS component can either exist only in the direct link between the source mobile station and the destination mobile station or in the link between the source mobile station and the destination mobile station via a mobile relay (i.e., the double Rice fading scenario) [10] or in both links. Our amplify-and-forward relay fading channel model takes into consideration the LOS component only in the direct link between the source mobile station and the destination mobile station. The novelty in our approach is that, we model the envelope of the amplify-and-forward relay channel as a single-LOS double-scattering (SLDS) fading channel, i.e., the superposition of a deterministic LOS component and a zero-mean complex double Gaussian process. The PDF of the envelope of SLDS fading channels has been derived in [11]. However, other important statistical quantities like the PDF of the phase, LCR, and ADF have not been studied so far. Here, we present the integral expressions for these statistical quantities. Furthermore, the validity of the analytical expressions is confirmed with the help of a high-performance channel simulator. In addition, the results presented in this paper will provide sufficient evidence that the properties of SLDS fading channels are quite different from those of double Rayleigh and double Rice channels.

The rest of the paper is structured as follows: In Sect. 2, the reference model for amplify-and-forward SLDS fading channels is developed. Section 3 deals with the analysis of the statistical properties of SLDS fading processes. Section 4 confirms the validity of the analytical expressions presented in Sect. 3 by simulations. Finally, concluding remarks are given in Sect. 5.

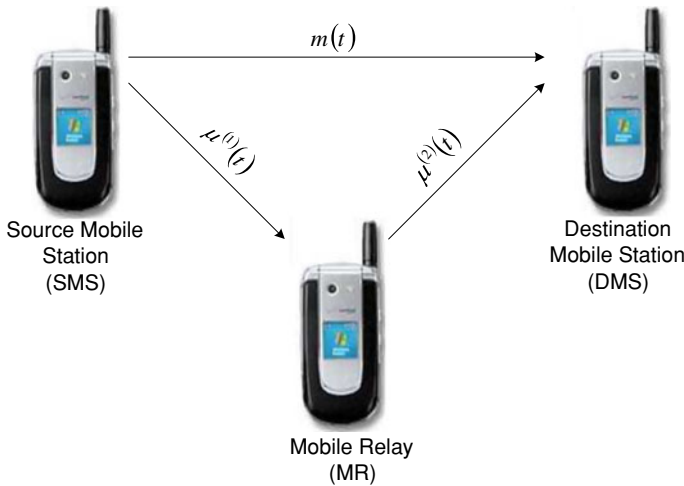


Fig. 1 The propagation scenario behind single-LOS double-scattering fading channels

2 The SLDS Fading Channel

In this section, we will develop a reference channel model for SLDS fading channels under the assumption of flat fading. It is important to note that SLDS fading channels are M2M fading channels in the amplify-and-forward relay links, where an LOS component exists only in the direct transmission link between the source mobile station and the destination mobile station. The communication scenario associated with SLDS fading channels is presented in Fig. 1.

Let us denote the transmission link between the source mobile station and the destination mobile station via the mobile relay as L_{S-R-D} . The signal transmitted by the source mobile station is $s(t)$. Furthermore, the deterministic LOS component, $m(t)$ defined as

$$m(t) = m_r(t) + jm_i(t) = \rho e^{j(2\pi f_\rho t + \theta_\rho)} \tag{1}$$

assumes fixed values for the amplitude ρ , Doppler frequency f_ρ , and phase θ_ρ . The Doppler frequency f_ρ of the LOS component corresponds to the sum of the Doppler frequencies f_{ρ_S} and f_{ρ_D} caused by the motion of the source mobile station and the destination mobile station, respectively, i.e., $f_\rho = f_{\rho_S} + f_{\rho_D}$. Throughout this paper, we will use the subscripts r and i to indicate the real and the imaginary part, respectively, of a complex number. The transmitted signal $s(t)$ following the link L_{S-R-D} reaches the destination mobile station in two steps. First, the signal $s(t)$ arrives through multipath propagation at the mobile relay, and then it is retransmitted to the destination mobile station. The signal $r_R(t)$ received by the mobile relay can be expressed as

$$r_R(t) = \mu^{(1)}(t) s(t) + n_1(t) \tag{2}$$

where $\mu^{(1)}(t)$ is a scattered component that describes the fading in the link between the source mobile station and the mobile relay (i.e., L_{S-R}), and $n_1(t)$ is an additive white Gaussian noise (AWGN) process. Here, the scattered component $\mu^{(1)}(t)$ is modeled as a zero-mean complex Gaussian process having $2\sigma_1^2$ variance, i.e., $\mu^{(1)}(t) = \mu_r^{(1)}(t) + j\mu_i^{(1)}(t)$. The mobile relay then amplifies the signal $r_R(t)$ and retransmits it to the destination mobile station. Thus, the total signal $r_D(t)$ received at the destination mobile station can be written as

$$\begin{aligned}
 r_D(t) &= m(t) s(t) + A_R \mu^{(2)}(t) r_R(t) + n_2(t) \\
 &= m(t) s(t) + A_R \mu^{(2)}(t) \mu^{(1)}(t) s(t) + A_R \mu^{(2)}(t) n_1(t) + n_2(t) \\
 &= \left(m(t) + A_R \mu^{(2)}(t) \mu^{(1)}(t) \right) s(t) + A_R \mu^{(2)}(t) n_1(t) + n_2(t) \\
 &= (m(t) + A_R \zeta(t)) s(t) + A_R \mu^{(2)}(t) n_1(t) + n_2(t)
 \end{aligned} \tag{3}$$

where A_R is referred to as the relay gain, $\mu^{(2)}(t)$ is the second scattered component, $\zeta(t)$ corresponds to the double scattered component, and $n_2(t)$ is the second AWGN process. We have assumed fixed gain relays in our model, meaning that the relay gain A_R is a real constant. The scattered component $\mu^{(2)}(t)$ is a zero-mean complex Gaussian process with variance $2\sigma_2^2$, i.e., $\mu^{(2)}(t) = \mu_r^{(2)}(t) + j\mu_i^{(2)}(t)$. This process models the fading channel in the link between the mobile relay and the destination mobile station (i.e., L_{R-D}). The double scattered component $\zeta(t)$ defines the overall fading channel in the link L_{S-R-D} . It represents a zero-mean complex double Gaussian process, which is modeled as the product of two independent, zero-mean complex Gaussian processes $\mu^{(1)}(t)$ and $\mu^{(2)}(t)$, i.e., $\zeta(t) = \zeta_r(t) + j\zeta_i(t) = \mu^{(1)}(t) \mu^{(2)}(t)$. It should be pointed out here that the relay gain A_R acts as a scaling factor for the variance of $\mu^{(2)}(t)$, i.e., $2\sigma_{A_R}^2 = \text{Var}\{A_R \mu^{(2)}(t)\} = 2(A_R \sigma_2)^2$. In (3), the sum of the double scattered component $\zeta(t)$ and the LOS component $m(t)$ results in a non-zero-mean complex double Gaussian process $\chi(t)$, i.e., $\chi(t) = \chi_r(t) + j\chi_i(t) = A_R \zeta(t) + m(t)$. This process $\chi(t)$ models the overall fading channel between the source mobile station and the destination mobile station. The absolute value of $\chi(t)$ gives rise to an SLDS process $\Xi(t)$, i.e.,

$$\Xi(t) = |\chi(t)|. \tag{4}$$

Furthermore, the argument of $\chi(t)$ defines the phase process $\Theta(t)$, i.e.,

$$\Theta(t) = \arg\{\chi(t)\}. \tag{5}$$

3 Statistical Analysis of SLDS Fading Channels

In this section, we derive the analytical expressions for the statistical properties of SLDS channels introduced in Sect. 2. The main statistical quantities of interest include the mean value, variance, PDF of the envelope as well as the phase, LCR and ADF.

3.1 Joint PDF of SLDS Processes

The starting point for the derivation of the statistics of SLDS processes is the computation of the joint PDF $p_{\chi_r \chi_i \dot{\chi}_r \dot{\chi}_i}(u_r, u_i, \dot{u}_r, \dot{u}_i)$ of the stationary processes $\chi_r(t)$, $\chi_i(t)$, $\dot{\chi}_r(t)$, and $\dot{\chi}_i(t)$ at the same time t . Throughout this paper, the overdot indicates the time derivative. Applying the concept of transformation of random variables [12], we can write the joint PDF $p_{\chi_r \chi_i \dot{\chi}_r \dot{\chi}_i}(u_r, u_i, \dot{u}_r, \dot{u}_i)$ as follows

$$\begin{aligned}
 p_{\chi_r \chi_i \dot{\chi}_r \dot{\chi}_i}(u_r, u_i, \dot{u}_r, \dot{u}_i) &= \int_{-\infty}^{\infty} \int_{-\infty}^{\infty} \int_{-\infty}^{\infty} \int_{-\infty}^{\infty} d\dot{y}_i d\dot{y}_r dy_i dy_r |J|^{-1} \\
 &\quad \times P_{\mu_r^{(1)} \mu_i^{(1)} \dot{\mu}_r^{(1)} \dot{\mu}_i^{(1)} \mu_r^{(2)} \mu_i^{(2)} \dot{\mu}_r^{(2)} \dot{\mu}_i^{(2)}}(x_r, x_i, \dot{x}_r, \dot{x}_i, y_r, y_i, \dot{y}_r, \dot{y}_i)
 \end{aligned} \tag{6}$$

where $p_{\mu_r^{(1)} \mu_i^{(1)} \dot{\mu}_r^{(1)} \dot{\mu}_i^{(1)} \mu_r^{(2)} \mu_i^{(2)} \dot{\mu}_r^{(2)} \dot{\mu}_i^{(2)}}(x_r, x_i, \dot{x}_r, \dot{x}_i, y_r, y_i, \dot{y}_r, \dot{y}_i)$ is the joint PDF of the real and imaginary parts of $\mu^{(k)}(t)$ as well as their respective time derivatives $\dot{\mu}^{(k)}(t)$ ($k = 1, 2$). The quantity x_l is a function of $y_r, y_i, u_r,$ and u_i , with \dot{x}_l as a function of $\dot{y}_r, \dot{y}_i, \dot{u}_r,$ and \dot{u}_i for $l = r, i$. In (6), J denotes the Jacobian determinant. It is worth mentioning here that the processes $\chi_l(t), \dot{\chi}_l(t), \mu_l^{(1)}(t), \dot{\mu}_l^{(1)}(t), \mu_l^{(2)}(t),$ and $\dot{\mu}_l^{(2)}(t)$ ($l = r, i$) are uncorrelated in pairs. Taking into account that the underlying Gaussian processes and their time derivatives, i.e., $\mu_l^{(k)}(t),$ and $\dot{\mu}_l^{(k)}(t)$ ($k = 1, 2; l = r, i$) are statistically independent allows us to write $p_{\mu_r^{(1)} \mu_i^{(1)} \dot{\mu}_r^{(1)} \dot{\mu}_i^{(1)} \mu_r^{(2)} \mu_i^{(2)} \dot{\mu}_r^{(2)} \dot{\mu}_i^{(2)}}(x_r, x_i, \dot{x}_r, \dot{x}_i, y_r, y_i, \dot{y}_r, \dot{y}_i)$ as a product of $p_{\mu_r^{(1)} \mu_i^{(1)} \dot{\mu}_r^{(1)} \dot{\mu}_i^{(1)}}(x_r, x_i, \dot{x}_r, \dot{x}_i)$ and $p_{\mu_r^{(2)} \mu_i^{(2)} \dot{\mu}_r^{(2)} \dot{\mu}_i^{(2)}}(y_r, y_i, \dot{y}_r, \dot{y}_i)$. Furthermore, $p_{\mu_r^{(1)} \mu_i^{(1)} \dot{\mu}_r^{(1)} \dot{\mu}_i^{(1)}}(x_r, x_i, \dot{x}_r, \dot{x}_i)$ and $p_{\mu_r^{(2)} \mu_i^{(2)} \dot{\mu}_r^{(2)} \dot{\mu}_i^{(2)}}(y_r, y_i, \dot{y}_r, \dot{y}_i)$ can be expressed by the multivariate Gaussian distribution (see, e.g., [13, Eq. (3.2)]). Thus, substituting $p_{\mu_r^{(1)} \mu_i^{(1)} \dot{\mu}_r^{(1)} \dot{\mu}_i^{(1)}}(x_r, x_i, \dot{x}_r, \dot{x}_i)$ and $p_{\mu_r^{(2)} \mu_i^{(2)} \dot{\mu}_r^{(2)} \dot{\mu}_i^{(2)}}(y_r, y_i, \dot{y}_r, \dot{y}_i)$ in (6) and doing some lengthy algebraic computations results in

$$p_{\chi_r \dot{\chi}_r \dot{\chi}_i} (u_r, u_i, \dot{u}_r, \dot{u}_i) = \frac{1}{(2\pi)^2 \sigma_1^2 \sigma_{AR}^2} \int_0^\infty v e^{-\frac{1}{2\sigma_1^2} \left(\frac{g_1(u_r, u_i, \rho)}{v^2} \right)} e^{-\frac{1}{2\sigma_{AR}^2} v^2} e^{-\frac{1}{2\beta_1} \left(\frac{g_2(\dot{u}_r, \dot{u}_i, \rho)}{v^2} \right)} \frac{\beta_2}{\beta_1} e^{\frac{\beta_2}{\beta_1} \left(\frac{g_1(u_r, u_i, \rho)}{v^2} \frac{g_2(\dot{u}_r, \dot{u}_i, \rho)}{v^2} \right)} \frac{1}{\beta_2 g_1(u_r, u_i, \rho) + \beta_1 v^4} dv \tag{7}$$

where

$$g_1(u_r, u_i, \rho) = u_r^2 + u_i^2 + \rho^2 - 2\rho u_r \cos(2\pi f_\rho t + \theta) - 2\rho u_i \sin(2\pi f_\rho t + \theta) \tag{8a}$$

$$g_2(\dot{u}_r, \dot{u}_i, \rho) = \dot{u}_r^2 + \dot{u}_i^2 + (2\pi f_\rho \rho)^2 - 4\pi f_\rho \rho \dot{u}_i \cos(2\pi f_\rho t + \theta) + 4\pi f_\rho \rho \dot{u}_r \sin(2\pi f_\rho t + \theta) \tag{8b}$$

and

$$\beta_1 = 2(\sigma_1 \pi)^2 (f_{\max_S}^2 + f_{\max_R}^2), \quad \beta_2 = 2(\sigma_{AR} \pi)^2 (f_{\max_R}^2 + f_{\max_D}^2). \tag{9a,b}$$

In (9a,b), the quantity β_k ($k = 1, 2$) is the negative curvature of the autocorrelation function of the real and imaginary parts of $\mu^{(k)}(t)$ ($k = 1, 2$) presented here for the case of isotropic scattering [14]. Furthermore, β_k ($k = 1, 2$) is the characteristic quantity corresponding to M2M fading process [15]. The symbols $f_{\max_S}, f_{\max_R},$ and f_{\max_D} appearing in (9a,b) correspond to the maximum Doppler frequency caused by the motion of the source mobile station, the mobile relay, and the destination mobile station, respectively.

Starting from (7), the transformation of the Cartesian coordinates (u_r, u_i) into polar coordinates (z, θ) by means of $z = \sqrt{u_r^2 + u_i^2}$ and $\theta = \arctan(u_i/u_r)$ results after some lengthy algebraic manipulations in

$$p_{\Xi \dot{\Xi} \Theta \dot{\Theta}}(z, \dot{z}, \theta, \dot{\theta}; t) = \frac{z^2}{(2\pi)^2 \sigma_1^2 \sigma_{AR}^2} \int_0^\infty v e^{-\frac{1}{2\sigma_1^2} \left(\frac{z^2 + \rho^2}{v^2} \right)} e^{-\frac{v^2}{2\sigma_{AR}^2}} e^{\frac{z\rho \cos(\theta - 2\pi f_\rho t - \theta_\rho)}{\sigma_1^2 v^2}} e^{-\frac{1}{2} \left(\frac{v^2 (\dot{z}^2 + (z\dot{\theta})^2) + (2\pi f_\rho v)^2}{\beta_2 g_3(z, \rho, \theta) + \beta_1 v^4} \right)} e^{\frac{2\pi f_\rho \rho v^2 (\dot{z} \sin(\theta - 2\pi f_\rho t - \theta_\rho) + z\dot{\theta} \cos(\theta - 2\pi f_\rho t - \theta_\rho))}{\beta_2 g_3(z, \rho, \theta) + \beta_1 v^4}} dv \tag{10}$$

for $z \geq 0$, $|\theta| \leq \pi$, $|\dot{z}| < \infty$, and $|\dot{\theta}| < \infty$. In (10), the function $g_3(\cdot, \cdot, \cdot)$ can be expressed as follows

$$g_3(z, \rho, \theta) = z^2 + \rho^2 - 2z\rho \cos(\theta - 2\pi f_\rho t - \theta_\rho). \quad (11)$$

The joint PDF $p_{\Xi \dot{\Xi} \Theta \dot{\Theta}}(z, \dot{z}, \theta, \dot{\theta}; t)$ in (10) is a fundamental equation, because it provides the basis for the computation of the PDF, LCR, and ADF of SLDS processes $\Xi(t)$, as well as the PDF of the phase process $\Theta(t)$. We will provide sufficient evidence in the rest of the current section to support our argument by deriving integral expressions for the PDFs, LCR, and ADF using (10).

3.2 PDF of SLDS Processes

The PDF $p_{\Xi}(z)$ of SLDS processes $\Xi(t)$ can be derived from (10) by solving the integrals over the joint PDF $p_{\Xi \dot{\Xi} \Theta \dot{\Theta}}(z, \dot{z}, \theta, \dot{\theta}; t)$ according to

$$p_{\Xi}(z) = \int_{-\pi}^{\pi} \int_{-\infty}^{\infty} \int_{-\infty}^{\infty} p_{\Xi \dot{\Xi} \Theta \dot{\Theta}}(z, \dot{z}, \theta, \dot{\theta}; t) d\dot{\theta} d\dot{z} d\theta, \quad z \geq 0. \quad (12)$$

The closed-form solution of (12) can be given as

$$p_{\Xi}(z) = \begin{cases} \frac{z}{\sigma_1^2 \sigma_{AR}^2} I_0\left(\frac{z}{\sigma_1 \sigma_{AR}}\right) K_0(\kappa), & z < \rho \\ \frac{z}{\sigma_1^2 \sigma_{AR}^2} K_0\left(\frac{z}{\sigma_1 \sigma_{AR}}\right) I_0(\kappa), & z \geq \rho \end{cases} \quad (13)$$

where $\kappa = \rho/(\sigma_1 \sigma_{AR})$, $I_0(\cdot)$ and $K_0(\cdot)$ are denoting the zeroth-order modified Bessel function of the first kind and the second kind [16], respectively. The PDF $p_{\Xi}(z)$ of SLDS processes $\Xi(t)$ presented in (13) can be verified from the literature (see, e.g., [11]).

The condition $\rho = 0$ indicates the absence of the LOS component in the direct link from the source mobile station to the destination mobile station. The PDF $p_{\Xi}(z)$ of SLDS processes $\Xi(t)$ given in (13) then reduces to the PDF of the envelope of double Rayleigh processes [17], i.e.,

$$p_{\Xi}(z) |_{\rho=0} = \frac{z}{\sigma_1^2 \sigma_{AR}^2} K_0\left(\frac{z}{\sigma_1 \sigma_{AR}}\right), \quad z \geq 0. \quad (14)$$

Furthermore, using the asymptotic expansions of the zeroth-order modified Bessel function of the first kind and the second kind, i.e., $I_0(\cdot)$ and $K_0(\cdot)$, respectively, [17], the PDF $p_{\Xi}(z)$ of SLDS processes $\Xi(t)$ in (13) can be approximated for large values of κ as the Laplace distribution [18], i.e.,

$$p_{\Xi}(z) |_{\kappa \gg 1} \approx \sqrt{\frac{z}{\rho}} \frac{1}{2\sigma_1 \sigma_{AR}} e^{-\frac{|z-\rho|}{\sigma_1 \sigma_{AR}}} \approx \sqrt{\frac{z}{\rho}} p_\rho(z), \quad z \geq 0 \quad (15)$$

where $p_\rho(z)$ represents the Laplace distribution having the mean value ρ and the variance $\sigma_1^2 \sigma_{AR}^2$. It is important to note here that the approximation in (15) is valid if $\kappa \gg 1$, i.e., the ratio of the power of the LOS component to the power of the scattered components is large. Otherwise, in the presence of a very strong LOS component, i.e., $\rho \gg 1$, when the power of the scattered components is constant, κ acquires a large value.

3.3 Mean Value and Variance of SLDS Processes

The expected value and the variance of a stochastic process are important statistical parameters, since they summarize the information provided by the PDF. The expected value m_{Ξ} of SLDS processes $\Xi(t)$ can be obtained using [12]

$$m_{\Xi} = E\{\Xi(t)\} = \int_{-\infty}^{\infty} z p_{\Xi}(z) dz \tag{16}$$

where $E\{\cdot\}$ is the expected value operator. Substituting (13) in (16) results in the following final expression

$$m_{\Xi} = \kappa K_0(\kappa) \left[\rho I_1(\kappa) + \frac{\pi}{2} \sigma_1 \sigma_{A_R} \{I_0(\kappa) L_1(\kappa) - I_1(\kappa) L_0(\kappa)\} \right] + \frac{I_0(\kappa)}{(\sigma_1 \sigma_{A_R})^2} g_4(z) \tag{17}$$

where

$$g_4(z) = \int_{\rho}^{\infty} z^2 K_0\left(\frac{z}{\sigma_1 \sigma_{A_R}}\right) dz. \tag{18}$$

In (17), $I_n(\cdot)$ and $K_n(\cdot)$ denote the n th-order modified Bessel functions of the first and the second kind [16], respectively, and $L_n(\cdot)$ designates the n th-order modified Struve function [16].

The difference of the mean power m_{Ξ^2} and the squared mean value $(m_{\Xi})^2$ of SLDS processes $\Xi(t)$ defines its variance σ_{Ξ}^2 [12], i.e.,

$$\sigma_{\Xi}^2 = \text{Var}\{\Xi(t)\} = m_{\Xi^2} - (m_{\Xi})^2. \tag{19}$$

By using (13) and [12, Eq. (5.67)], the mean power m_{Ξ^2} of SLDS processes $\Xi(t)$ can be expressed as

$$\begin{aligned} m_{\Xi^2} &= E\{\Xi^2(t)\} = \int_{-\infty}^{\infty} z^2 p_{\Xi}(z) dz \\ &= 2\rho^2 K_0(\kappa) \left(I_2(\kappa) + \frac{\kappa}{2} I_3(\kappa) \right) + \frac{I_0(\kappa)}{(\sigma_1 \sigma_{A_R})^2} g_5(z) \end{aligned} \tag{20}$$

where the function $g_5(\cdot)$ is defined as follows

$$g_5(z) = \int_{\rho}^{\infty} z^3 K_0\left(\frac{z}{\sigma_1 \sigma_{A_R}}\right) dz. \tag{21}$$

From (17), (20), and by using (19), the variance σ_{Ξ}^2 of SLDS processes $\Xi(t)$ can easily be calculated.

3.4 PDF of Phase Processes

The PDF $p_{\Theta}(\theta; t)$ of phase processes $\Theta(t)$ can be derived from (10) by solving the integrals over the joint PDF $p_{\Xi\dot{\Xi}\Theta\dot{\Theta}}(z, \dot{z}, \theta, \dot{\theta}; t)$ according to

$$p_{\Theta}(\theta; t) = \int_0^{\infty} \int_{-\infty}^{\infty} \int_{-\infty}^{\infty} p_{\Xi\dot{\Xi}\Theta\dot{\Theta}}(z, \dot{z}, \theta, \dot{\theta}; t) d\dot{\theta} d\dot{z} dz, \quad |\theta| \leq \pi. \tag{22}$$

This results in the following final expression

$$p_{\Theta}(\theta; t) = \frac{1}{2\pi} \int_0^{\infty} dx e^{-x - \frac{1}{x} \left(\frac{\rho}{2\sigma_{AR}} \right)^2} \left[1 + \sqrt{\frac{\pi}{2}} g_6(x, \rho, f_{\rho}, \theta) \right. \\ \left. \times e^{\frac{1}{2} g_6(x, \rho, f_{\rho}, \theta)^2} \left\{ 1 + \Phi \left(\frac{g_6(x, \rho, f_{\rho}, \theta)}{\sqrt{2}} \right) \right\} \right], \quad |\theta| \leq \pi \tag{23}$$

where

$$g_6(x, \rho, \theta) = \frac{\rho \cos(\theta - 2\pi f_{\rho} t - \theta_{\rho})}{\sigma_{AR} \sqrt{2x}}. \tag{24}$$

Furthermore, in (23), $\Phi(\cdot)$ represents the error function [16, Eq. (8.250.1)]. From (23), it is obvious that the phase process $\Theta(t)$ is not stationary in a strict sense since $p_{\Theta}(\theta; t) \neq p_{\Theta}(\theta)$. This time dependency of the PDF $p_{\Theta}(\theta; t)$ is due the Doppler frequency f_{ρ} of the LOS component $m(t)$. However, for the special case that $f_{\rho} = 0$ ($\rho \neq 0$), the phase process $\Theta(t)$ is a strict sense stationary process. As $\rho \rightarrow 0$, it follows $\Xi(t) = |\zeta(t) + m(t)| \rightarrow |\zeta(t)|$, and from (23), we obtain the uniform distribution

$$p_{\Theta}(\theta) |_{\rho=0} = \frac{1}{2\pi}, \quad -\pi < \theta \leq \pi. \tag{25}$$

3.5 LCR of SLDS Processes

The LCR of the envelope of mobile fading channels is a measure to describe the average number of times the envelope crosses a certain threshold level r from up to down (or vice versa) per second. The LCR $N_{\Xi}(r)$ of SLDS processes $\Xi(t)$ can be obtained using [19]

$$N_{\Xi}(r) = \int_0^{\infty} \dot{z} p_{\Xi\dot{\Xi}}(r, \dot{z}) d\dot{z} \tag{26}$$

where $p_{\Xi\dot{\Xi}}(r, \dot{z})$ is the joint PDF of SLDS processes $\Xi(t)$ and its corresponding time derivative $\dot{\Xi}(t)$ at the same time t . The joint PDF $p_{\Xi\dot{\Xi}}(z, \dot{z})$ can be derived from (10) by solving the integrals over the joint PDF $p_{\Xi\dot{\Xi}\Theta\dot{\Theta}}(z, \dot{z}, \theta, \dot{\theta}; t)$ according to

$$p_{\Xi\dot{\Xi}}(z, \dot{z}) = \int_{-\pi}^{\pi} \int_{-\infty}^{\infty} p_{\Xi\dot{\Xi}\Theta\dot{\Theta}}(z, \dot{z}, \theta, \dot{\theta}; t) d\dot{\theta} d\theta, \quad z \geq 0, |\dot{z}| \leq \infty. \tag{27}$$

After, some lengthy computations, the joint PDF in (27) results in the following expression

$$\begin{aligned}
 p_{\Xi\dot{\Xi}}(z, \dot{z}) = & \frac{\sqrt{2\pi} z}{(2\pi)^2 \sigma_1^2 \sigma_{AR}^2} \int_0^\infty \int_{-\pi}^\pi e^{-\frac{1}{2\sigma_1^2} \left(\frac{z^2 + \rho^2}{v^2} \right)} e^{-\frac{v^2}{2\sigma_{AR}^2}} e^{\frac{z\rho \cos \theta}{v^2 \sigma_1^2}} e^{-\frac{2(\pi f \rho \rho v \sin \theta)^2}{\beta_2 g_7(z, \rho, \theta) + \beta_1 v^4}} \\
 & \times e^{-\frac{1}{2} \left(\frac{(v\dot{z})^2 - 4\pi f \rho \rho v^2 \dot{z} \sin \theta}{\beta_2 g_7(z, \rho, \theta) + \beta_1 v^4} \right)} d\theta dv, \quad z \geq 0, |\dot{z}| \leq \infty
 \end{aligned} \tag{28}$$

where

$$g_7(z, \rho, \theta) = z^2 + \rho^2 - 2z\rho \cos \theta. \tag{29}$$

Finally, after substituting (28) in (26) and doing some extensive mathematical manipulations, the LCR $N_\Xi(r)$ of SLDS processes $\Xi(t)$ can be expressed as follows

$$\begin{aligned}
 N_\Xi(r) = & \frac{\sqrt{2\pi} r}{(2\pi)^2 \sigma_1^2 \sigma_{AR}^2} \int_0^\infty \int_{-\pi}^\pi d\theta dv \frac{\sqrt{\beta_2 g_7(r, \rho, \theta) + \beta_1 v^4}}{v^2} e^{-\frac{v^2}{2\sigma_{AR}^2}} e^{-\frac{g_7(r, \rho, \theta)}{2v^2 \sigma_1^2}} \\
 & \times \left(e^{-\frac{1}{2} g_8^2(r, v, \rho, \theta)} + \sqrt{\frac{\pi}{2}} g_8(r, v, \rho, \theta) \left[1 + \Phi \left(\frac{g_8(r, v, \rho, \theta)}{\sqrt{2}} \right) \right] \right)
 \end{aligned} \tag{30}$$

where

$$g_8(r, v, \rho, \theta) = \frac{2\pi f \rho \rho v \sin \theta}{\sqrt{\beta_2 g_7(r, \rho, \theta) + \beta_1 v^4}}. \tag{31}$$

The quantities β_1 and β_2 are the same as those defined in (9a,b). Furthermore, $g_7(\cdot, \cdot, \cdot)$ is the function defined in (29).

Considering the special case when $\rho = 0$, (30) reduces to the expression of the LCR for double Rayleigh processes given in [7] as

$$N_\Xi(r) |_{\rho=0} = \frac{r}{\sqrt{2\pi} \sigma_1^2 \sigma_{AR}^2} \int_0^\infty \frac{\sqrt{\beta_2 r^2 + \beta_1 v^4}}{v^2} e^{-\frac{(r/v)^2}{2\sigma_1^2}} e^{-\frac{v^2}{2\sigma_{AR}^2}} dv. \tag{32}$$

3.6 ADF of SLDS Processes

We will conclude Sect. 3 with the discussion on the ADF. The ADF $T_{\Xi-}(r)$ of SLDS processes $\Xi(t)$ can be defined as the ratio of the CDF $F_{\Xi-}(r)$ of $\Xi(t)$ and its LCR $N_\Xi(r)$, i.e.,

$$T_{\Xi-}(r) = \frac{F_{\Xi-}(r)}{N_\Xi(r)}. \tag{33}$$

The CDF $F_{\Xi-}(r)$ of SLDS processes $\Xi(t)$ can be expressed using (13) as follows

$$\begin{aligned}
 F_{\Xi-}(r) = & \int_0^r p_\Xi(z) dz \\
 = & \begin{cases} \frac{r}{\sigma_1 \sigma_{AR}} K_0(\kappa) I_1 \left(\frac{r}{\sigma_1 \sigma_{AR}} \right), & r < \rho \\ 1 - \frac{r}{\sigma_1 \sigma_{AR}} I_0(\kappa) K_1 \left(\frac{r}{\sigma_1 \sigma_{AR}} \right), & r \geq \rho. \end{cases}
 \end{aligned} \tag{34}$$

From (34), (30), and by using (33), the ADF $T_{\Xi_-}(r)$ of SLDS processes $\Xi(t)$ can easily be computed.

It is quite obvious from (34) that as $\rho \rightarrow 0$, (34) reduces to

$$F_{\Xi_-}(r) \Big|_{\rho=0} = 1 - \frac{r}{\sigma_1 \sigma_{A_R}} K_1 \left(\frac{r}{\sigma_1 \sigma_{A_R}} \right). \quad (35)$$

The resulting CDF $F_{\Xi_-}(r)$ in (35) corresponds to the CDF of double Rayleigh processes [8]. Thus, substituting (35) and (32) in (33) gives the ADF of double Rayleigh processes.

4 Numerical Results

In this section, we will confirm the correctness of the analytical expressions presented in Sect. 3 with the help of simulations. Furthermore, for a detailed analysis the results for SLDS processes are compared with those of classical Rayleigh, classical Rice, double Rayleigh, and double Rice processes. It is important to note that the double Rice process is defined as the product of two independent classical Rice processes, i.e., $\Xi(t) = |\mu^{(1)}(t) + \rho_1| |\mu^{(2)}(t) + \rho_2|$. To simplify matters, the amplitudes ρ_1 and ρ_2 of the LOS components of the double Rice process are considered to be equal, i.e., $\rho_1 = \rho_2 = \rho$. The concept of sum-of-sinusoids (SOS) [14] is used to simulate uncorrelated complex Gaussian processes $\mu^{(k)}(t)$ that make up the overall SLDS process. For simulating Gaussian processes $\mu^{(k)}(t)$, $N_l^{(k)} = 20$ ($k = 1, 2$; $l = r, i$) is used. Here, $N_r^{(k)}$ and $N_i^{(k)}$ denote the number of sinusoids required to generate the real and the imaginary parts of $\mu^{(k)}(t)$, respectively. It is readily available in the literature that $N_l^{(k)} \geq 7$ is a sufficient number to approximate the simulated distribution of $|\mu^{(k)}(t)|$ very close to the Rayleigh distribution [14]. For the computation of the model parameters, we selected the generalized method of exact Doppler spread (GMEDS_q) proposed in [20] for $q = 1$. The values for the maximum Doppler frequencies f_{\max_S} , f_{\max_R} , and f_{\max_D} were set to 91 Hz, 75 Hz, and 110 Hz, respectively. The relay gain A_R as well as the parameters σ_1 and σ_2 were selected to be 1, unless stated otherwise.

The results presented in Figs. 2, 3, 4, 5, 6, 7, 8, and 9 show an excellent fitting of the analytical and the simulation results. In Fig. 2, the PDF $p_{\Xi}(z)$ of SLDS processes $\Xi(t)$ is being compared with those of classical Rice and double Rice processes for different values of ρ , where f_{ρ} was set to zero. It can be observed that the maximum value of the PDF $p_{\Xi}(z)$ of SLDS processes $\Xi(t)$ is higher than that of classical Rice and double Rice processes for same value of ρ . On the other hand, the spread of the PDF $p_{\Xi}(z)$ of SLDS processes $\Xi(t)$ follows the same trend as that of classical Rayleigh, classical Rice, and double Rayleigh processes. However, the PDF $p_{\Xi}(z)$ of the SLDS process $\Xi(t)$ has a narrower spread when compared to the spread of double Rice processes for the same value of ρ .

Figure 3 demonstrates the fact that for increasing values of κ , the PDF $p_{\Xi}(z)$ of SLDS processes $\Xi(t)$ approaches the symmetrical Laplace distribution. Furthermore, the right shift of the PDF $p_{\Xi}(z)$ of SLDS processes $\Xi(t)$ with increasing values of ρ is merely due to the fact that ρ contributes towards the mean value of SLDS processes. The mean value of SLDS processes for different values of ρ is presented in Fig. 4 along with the mean value of classical Rice and double Rice processes. It is obvious from Fig. 4 that the increase in the mean value of classical Rice and SLDS processes is proportional to ρ , whereas for double Rice processes it is proportional to the squared value of ρ .

The observation that the PDF $p_{\Xi}(z)$ of SLDS processes $\Xi(t)$ has a narrower spread when compared to the spread of double Rice processes is more explicitly shown in Fig. 5. In Fig. 5,

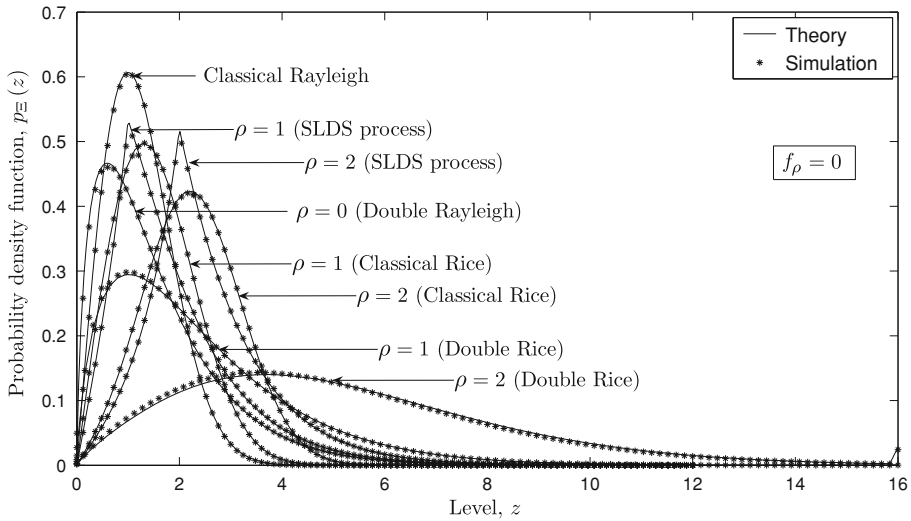


Fig. 2 A comparison of the PDF $p_{\Xi}(z)$ of SLDS processes $\Xi(t)$ with that of various other stochastic processes

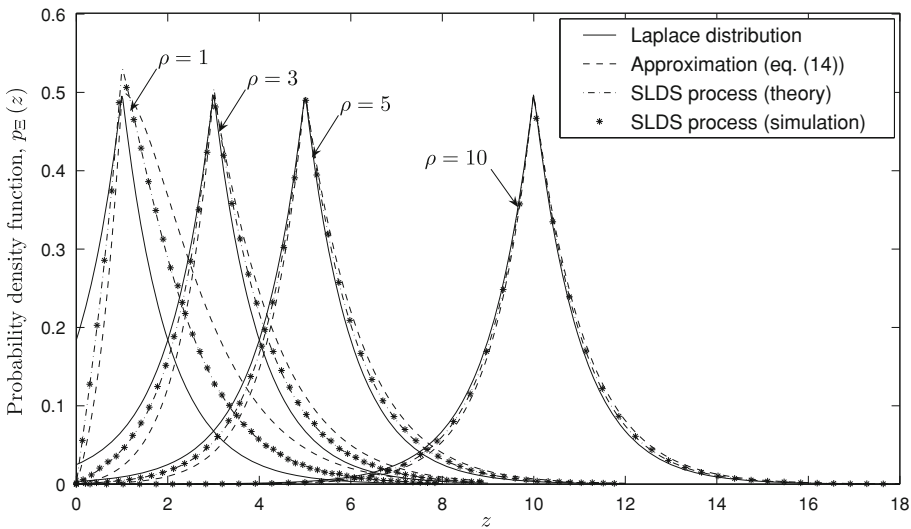


Fig. 3 Approximation of the PDF $p_{\Xi}(z)$ of SLDS processes $\Xi(t)$ to the Laplace distribution

the standard deviation σ_{Ξ} of SLDS processes $\Xi(t)$ for different values of ρ is presented along with the standard deviation of classical Rice and double Rice processes. It can be seen from Fig. 5 that for a particular value of ρ the standard deviation corresponding to double Rice processes is greater than that of classical Rice and SLDS processes. Furthermore, when the standard deviation σ_{Ξ} of various stochastic processes, i.e., the classical Rice, the double Rice, and the SLDS process is self-compared for different values of ρ , it can be observed in Fig. 5 that there is no noticeable difference in the standard deviation σ_{Ξ} of classical Rice and SLDS processes with increasing values of ρ . However, the increase in the standard deviation of double Rice processes, meaning thereby an increase in the spread of the PDF of these

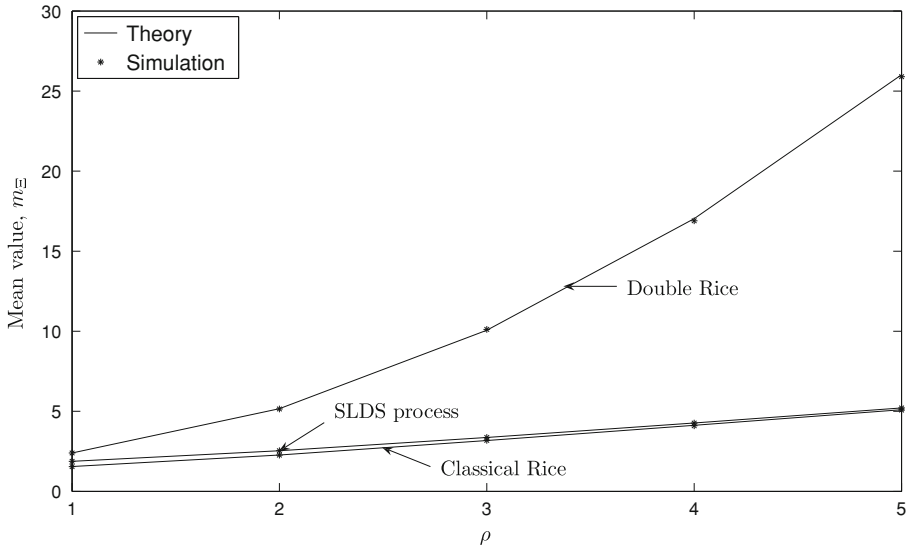


Fig. 4 A comparison of the mean value m_{Ξ} of SLDS processes $\Xi(t)$ with that of various other stochastic processes

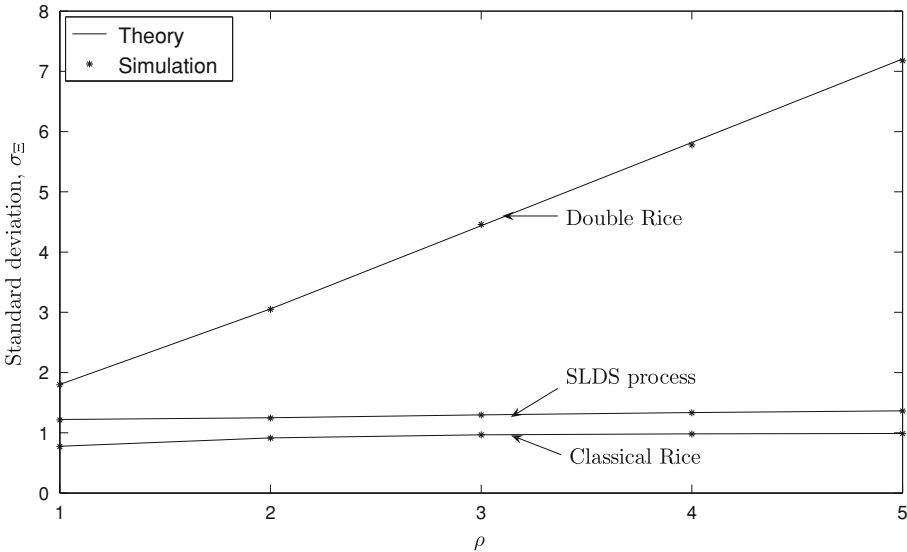


Fig. 5 A comparison of the standard deviation σ_{Ξ} of SLDS processes $\Xi(t)$ with that of various other stochastic processes

processes with increasing ρ is quite obvious. Similarly, Fig. 6 presents the CDF $F_{\Xi}(r)$ of SLDS processes $\Xi(t)$ evaluated by using (34).

A comparison of the PDF $p_{\Theta}(\theta)$ of the phase process $\Theta(t)$ with that of the corresponding classical Rice and double Rice phase processes is shown in Fig. 7. It is clear from Fig. 7 that the PDF $p_{\Theta}(\theta)$ of the phase process $\Theta(t)$ has a higher peak and narrow spread when

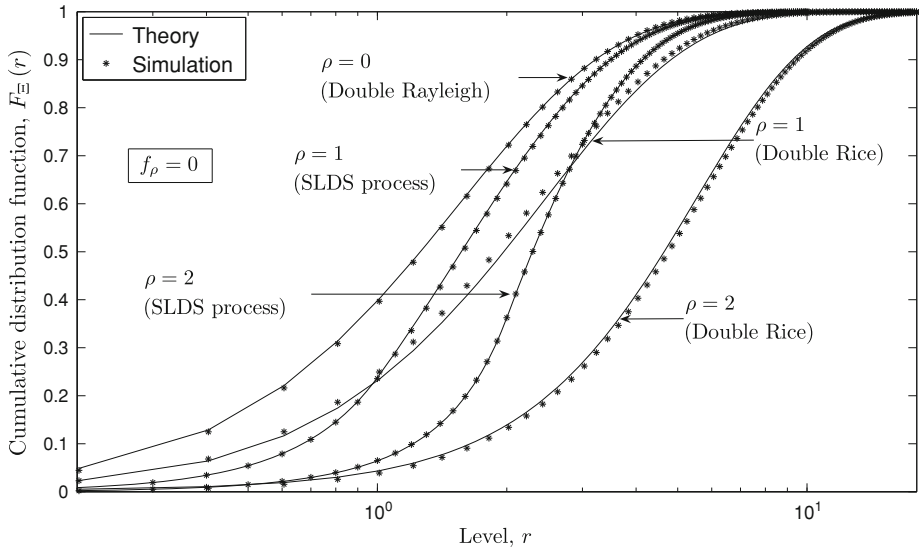


Fig. 6 A comparison of the CDF $F_{\Xi}(r)$ of SLDS processes $\Xi(t)$ with that of various other stochastic processes

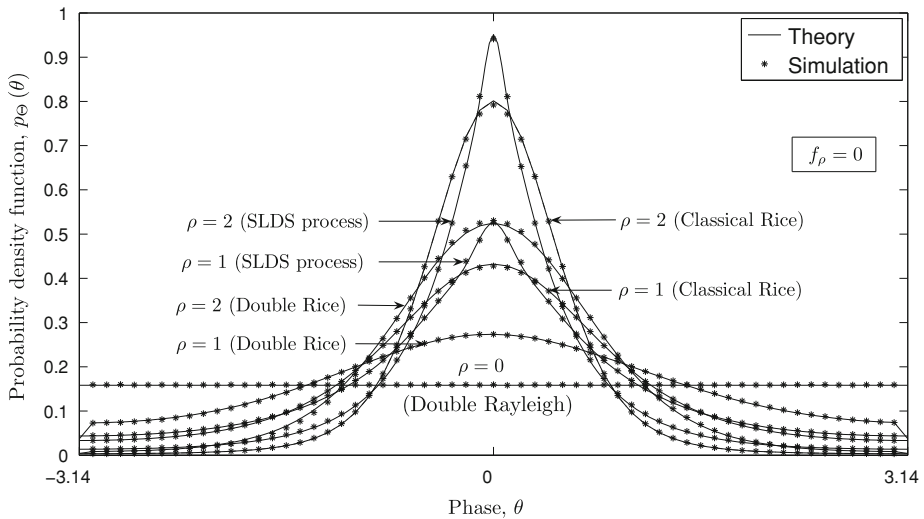


Fig. 7 A comparison of the PDF $p_{\Theta}(\theta)$ of the phase process $\Theta(t)$ with that of various other stochastic processes

compared with the PDF of the phase process associated with classical Rice and double Rice processes for a specific value of ρ .

Figure 8 shows that at low signal levels, the LCR $N_{\Xi}(r)$ of SLDS processes $\Xi(t)$ decreases with an increase in ρ , keeping f_{ρ} constant. While, $N_{\Xi}(r)$ increases at medium and high levels with increasing ρ . Furthermore, as ρ increases, the LCR $N_{\Xi}(r)$ of SLDS processes $\Xi(t)$ becomes higher than that of double Rice processes at low signal levels. However, at medium

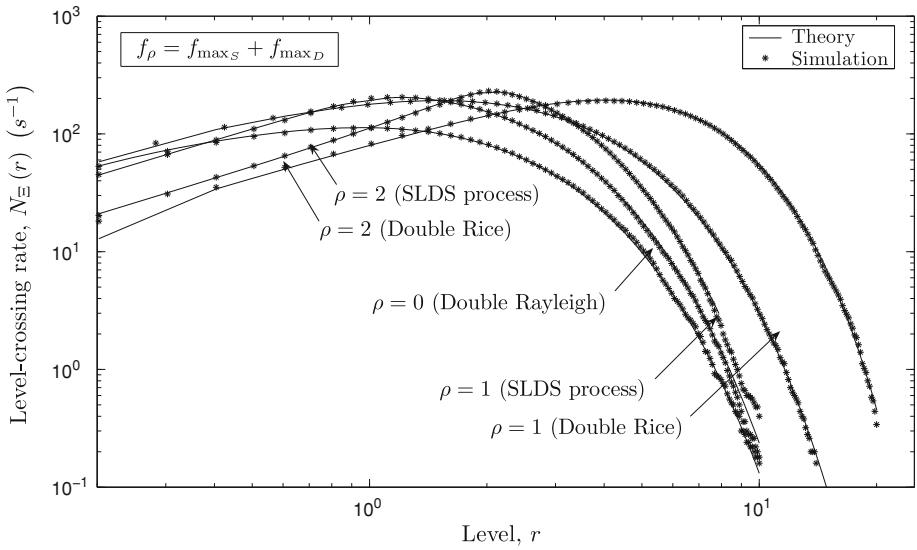


Fig. 8 A comparison of the LCR $N_{\Xi}(r)$ of SLDS processes $\Xi(t)$ for various values of ρ with that of various other stochastic processes

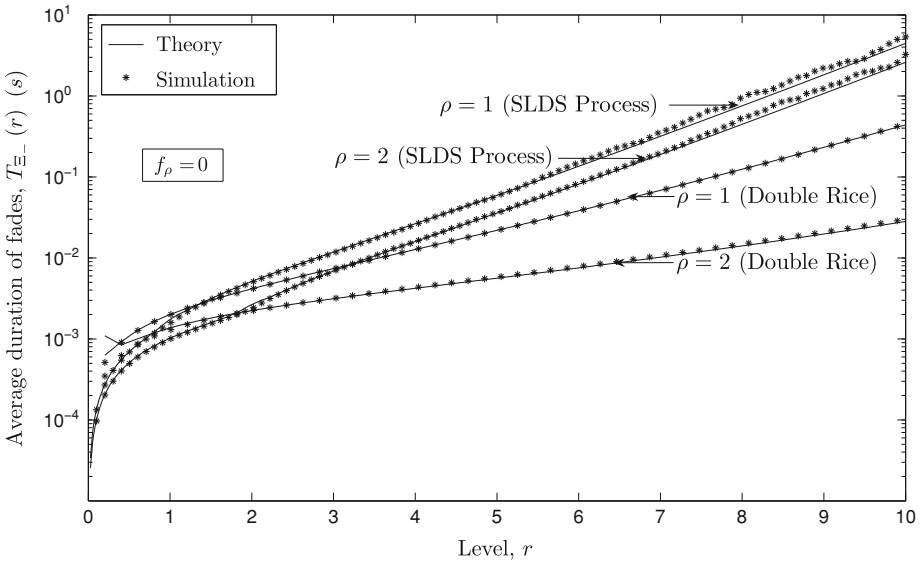


Fig. 9 A comparison of the ADF $T_{\Xi-}(r)$ of SLDS processes $\Xi(t)$ for various values of ρ with that of various other stochastic processes

and high signal levels, the LCR $N_{\Xi}(r)$ of SLDS processes $\Xi(t)$ is lower than the LCR of double Rice processes for the same value of ρ . Similarly, Fig. 9 compares the ADF $T_{\Xi-}(r)$ of SLDS processes $\Xi(t)$ with that of double Rice processes for different values of ρ keeping f_{ρ} equal to zero.

5 Conclusion

In this paper, we have studied the statistics of M2M fading channels in cooperative wireless networks under LOS conditions. Considering the amplify-and-forward relay type systems, the existence of an LOS component in the direct transmission link between the source mobile station and the destination mobile station results in SLDS fading channels. Here, we have modeled the NLOS link of the system as a zero-mean complex double Gaussian channel. Thus, the overall SLDS fading channel is modeled as the superposition of a deterministic LOS component and the zero-mean complex double Gaussian channel.

Statistical properties of SLDS fading channels are thoroughly investigated in this paper. We have derived analytical expressions for the mean, variance, PDFs, LCR, and ADF. Furthermore, we have verified our analytical expressions using numerical techniques in simulations. The close fitting of the presented theoretical and simulation results proves correctness of our analytical expressions. It has been shown that the properties of SLDS processes are quite different from both double Rayleigh and the double Rice processes. For example, the PDF of SDLS processes approaches the symmetrical Laplace distribution when the amplitude of the LOS component increases. Furthermore, the PDF of SLDS processes has a higher maximum value as compared to various other stochastic processes. On the other hand, for a particular value of ρ , the spread of the PDF of SLDS processes, follows the same trend as that of classical Rayleigh and classical Rice processes. However, the PDF of SLDS processes has a narrower spread as compared to the spread of double Rice processes. With increasing values of ρ the PDF of the phase process associated with SLDS processes acquires a higher maximum value and a narrower spread. A thorough analysis of the LCR of SLDS processes reveals that at low signal levels, the LCR of SLDS processes decreases when ρ increases. However, the LCR of SLDS processes increases with increasing ρ at low signal levels, when compared with the LCR of double Rice processes. At medium and high signal levels, the LCR of SLDS processes is always lower than that of double Rice processes for the same value of ρ . The ADF of SLDS processes shows a behavior opposite to the LCR of SLDS processes. We have also provided sufficient evidence in this paper that SLDS processes reduce to double Rayleigh processes in the absence of the LOS component.

The theoretical analysis presented in this paper is useful for researchers and designers of the physical layer for mobile-to-mobile communication systems. Our study provides an insight into the dynamics of SLDS fading channels, which can be exploited to develop robust modulation and coding schemes for such fading environments. Furthermore, with the help of the designed channel simulator, the overall performance of the system can also be evaluated by simulation for different kinds of SLDS fading environments.

References

1. Sendonaris, A., Erkip, E., & Aazhang, B. (2003). User cooperation diversity—Part I: System description. *IEEE Transactions on Communications*, 51(11), 1927–1938.
2. Sendonaris, A., Erkip, E., & Aazhang, B. (2003). User cooperation diversity—Part II: Implementation aspects and performance analysis. *IEEE Transactions on Communications*, 51(11), 1939–1948.
3. Laneman, J. N., Tse, D. N. C., & Wornell, G. W. (2004). Cooperative diversity in wireless networks: Efficient protocols and outage behavior. *IEEE Transactions on Information Theory*, 50(12), 3062–3080.
4. Akki, A. S., & Haber, F. (1986). A statistical model of mobile-to-mobile land communication channel. *IEEE Transactions on Vehicular Technology*, 35(1), 2–7.
5. Dohler, M. (2003). *Virtual antenna arrays*. Ph.D. dissertation, King's College, London, UK.

6. Barbarossa, S., & Scutari, G. (2003). Cooperative diversity through virtual arrays in multihop networks. In *Proceedings of the IEEE international conference on acoustics, speech, signal processing* (pp. 209–212). Hong Kong, China.
7. Patel, C. S., Stüber, G. L., & Pratt, T. G. (2006). Statistical properties of amplify and forward relay fading channels. *IEEE Transactions on Vehicular Technology*, 55(1), 1–9.
8. Kovacs, I. Z., Eggers, P. C. F., Olesen, K., & Petersen, L. G. (2002). Investigations of outdoor-to-indoor mobile-to-mobile radio communications channels. In *Proceedings of the IEEE 56th vehicle technology conference, VTC'02-Fall* (pp. 430–434). Vancouver, BC, Canada.
9. Salo, J., El-Sallabi, H. M., & Vainikainen, P. (2006). Impact of double-Rayleigh fading on system performance. In *Proceedings of the 1st IEEE international symposium on wireless pervasive computing, ISWPC 2006*. Phuket, Thailand (0-7803-9410-0/10.1109/ISWPC.2006.1613574).
10. Talha, B., & Pätzold, M. (2007). On the statistical properties of double Rice channels. In *Proceedings of the 10th international symposium on wireless personal multimedia communications, WPMC 2007* (pp. 517–522). Jaipur, India.
11. Salo, J., El-Sallabi, H. M., & Vainikainen, P. (2006). Statistical analysis of the multiple scattering radio channel. *IEEE Transactions on Vehicular Technology*, 54(11), 3114–3124.
12. Papoulis, A., & Pillai, S. U. (2002). *Probability, random variables and stochastic processes* (4th ed.). New York: McGraw-Hill.
13. Simon, M. K. (2002). *Probability distributions involving Gaussian random variables: A handbook for engineers and scientists*. Dordrecht: Kluwer Academic Publishers.
14. Pätzold, M. (2002). *Mobile fading channels*. Chichester: Wiley.
15. Akki, A. S. (1994). Statistical properties of mobile-to-mobile land communication channels. *IEEE Transactions on Vehicular Technology*, 43(4), 826–831.
16. Gradshteyn, I. S., & Ryzhik, I. M. (2000). *Table of integrals, series, and products* (6th ed.). New York: Academic Press.
17. Watson, G. N. (1966). *A treatise on the theory of Bessel functions* (2nd ed.). Bentley House, London: Cambridge University Press.
18. Kotz, S., Kozubowski, T. J., & Podgórski, K. (2001). *The Laplace distribution and generalizations: A revisit with applications to communications, economics, engineering, and finance*. Boston: Birkhäuser.
19. Rice, S. O. (1945). Mathematical analysis of random noise. *The Bell System Technical Journal*, 24, 46–156.
20. Pätzold, M., & Hogstad, B. O. (2006). Two new methods for the generation of multiple uncorrelated Rayleigh fading waveforms. In *Proceedings of the IEEE 63rd semiannual vehicular technology conference, VTC'06-Spring* (Vol. 6, pp. 2782–2786). Melbourne, Australia.

Author Biographies



Batoool Talha was born in Rawalpindi, Pakistan, in 1981. She received her bachelor's degree (BE) in Electrical Engineering (EE) in 2003 from the National University of Engineering Sciences and Technology (NUST) in Rawalpindi, Pakistan, and master's degree (MS) in Telecommunications and Electronics in 2005 from the University of Gävle, Sweden. For her master's thesis, she worked on a project, established in cooperation with Aalborg University and Nokia Networks, Denmark. Afterwards she worked as a research assistance in Aalborg University and Nokia Networks, Denmark till March 2006. Since September 2006, she has been working on her PhD thesis under the supervision of Professor Matthias Pätzold at the University of Agder, Grimstad, Norway. One of her publications has received the best student paper award. She has also performed the duties of session chair in WPMC'07. Her current

research interests include mobile fading channel modeling for mobile-to-mobile communication systems.



Matthias Pätzold received the Dipl.-Ing. and Dr.-Ing. degrees in electrical engineering from Ruhr-University Bochum, Bochum, Germany, in 1985 and 1989, respectively, and the habil. degree in Communications Engineering from the Technical University of Hamburg-Harburg, Hamburg, Germany, in 1998. From 1990 to 1992, he was with ANT Nachrichtentechnik GmbH, Backnang, Germany, where he was engaged in Digital Satellite Communications. From 1992 to 2001, he was with the department of Digital Networks at the Technical University Hamburg-Harburg. Since 2001, he has been a full professor of Mobile Communications with the University of Agder, Grimstad, Norway. He authored several books and more than 150 technical papers. His publications received eight best paper awards. He has been actively participating in numerous conferences serving as TPC chair and TPC member for more than 10 conferences within the recent 2 years.